Elsevier Editorial System(tm) for Journal of Molecular Structure

Manuscript Draft

Manuscript Number:

Title: Geomtry optimization, UV/Vis, NBO, HOMO and LUMO, excited state and antioxidant evaluation of new pyrimidine derivatives

Article Type: Research Paper

Keywords: pyrimidine; UV/Vis spectrum; NBO; DFT; antioxidant activity; natural charge

Corresponding Author: Dr. Masoome Sheikhi, Ph.D

Corresponding Author's Institution: Young Researchers and Elite Club, Gorgan Branch, Islamic Azad University, Gorgan, Iran

First Author: Siyamak Shahab, Prof.

Order of Authors: Siyamak Shahab, Prof.; Masoome Sheikhi, Ph.D; Evgeni Kvasyuk, Ph.D; Aliaksei G. Sysa, Ph.D; Radwan Alnajjar, Ph.D; Aleksandra Strogova, Ms; Kseniya Sirotsina, Ms; Hanna Yurlevich, Ms; Darya Novik, Ms

Dated: January 26, 2020

To

The Editor

Journal of Molecular Structure

Subject: **Submission of Manuscript**

Respected Sir,

Please find attached herewith the manuscript entitled as "**Geomtry optimization, UV/Vis, NBO, HOMO and LUMO, excited state and antioxidant evaluation of new pyrimidine derivatives**" by Siyamak Shahab, Masoome Sheikhi, Evgeni Kvasyuk, Aliaksei G. Sysa, Radwan Alnajjar, Aleksandra Strogova, Kseniya Sirotsina, Hanna Yurlevich, Darya Novik for the publication in **Journal of Molecular Structure**. The current manuscript has not been previously published and not submitted for review to any other journal and will not be submitted elsewhere before a decision is made. It is certified that publication is approved by all authors.

Thanking You

With Regards

Dr. Masoome Sheikhi

Young Researchers and Elite Club, Gorgan Branch, Islamic Azad University, Gorgan, Iran

Corresponding author email address: m.sheikhi2@gmail.com

Highlights

- Study of Antioxidant propertyof the new pyrimidine derivatives
- The DPPH radical scavenging of the new pyrimidines
- Antioxidative Chemical Assays and in vitro anticancer activity of new pyrimidine
- DFT calculations was performed with B3LYP/6-31G* level of theory
- FMO, MEP, NBO and absorption spectrum analysis

*Manuscript
Click here to view linked References

Title Page Information

Dear Sir,

Submission of manuscript for full paper in Journal of Molecular Structure

Please find herewith the enclosed manuscript:

Article title

Geomtry optimization, UV/Vis, NBO, HOMO and LUMO, excited state and antioxidant evaluation of new pyrimidine derivatives

The name of journal

Journal of Molecular Structure

The author's affiliations with full postal address

Siyamak Shahab
Belarusian State University, ISEI BSU, Minsk, Republic of Belarus
E-mail: siyamak.shahab@yahoo.com

Masoome Sheikhi
Young Researchers and Elite Club, Gorgan Branch, Islamic Azad University, Gorgan, Iran
E-mail: m.sheikhi2@gmail.com

Evgeni Kvasyuk
Belarusian State University, ISEI BSU, Minsk, Republic of Belarus
E-mail: ekvasyuk@inbox.ru

A.G. Sysa (Aliaksei G. Sysa)
Belarusian State University, ISEI BSU, Minsk, Republic of Belarus
E-mail: Aliaksei.sysa@iseu.by

Radwan Alnajjar
Department of Chemistry, Faculty of Science, University of Benghazi, Benghazi, Libya.
Departmentof Chemistry, University of Cape Town, Rondebosch 7701, South Africa.
E-mail: Radwan.Alnajjar@uob.edu.ly

Aleksandra Strogova
Belarusian State University, ISEI BSU, Minsk, Republic of Belarus
E-mail:a_strogova@bk.ru

Kseniya Sirotsina
Belarusian State University, ISEI BSU, Minsk, Republic of Belarus
E-mail: zmeenosec15@gmail.com

Hanna Yurlevich
Belarusian State University, ISEI BSU, Minsk, Republic of Belarus
E-mail: ann.yurlevich@gmail.com

Darya Novik
Belarusian State University, ISEI BSU, Minsk, Republic of Belarus
E-mail: novik301199@gmail.com

Geomtry optimization, UV/Vis, NBO, HOMO and LUMO, excited state and antioxidant evaluation of new pyrimidine derivatives

Siyamak Shahab[a,b,c], Masoome Sheikhi[d], Evgeni Kvasyuk[a], Aliaksei G. Sysa[a], Radwan Alnajjar[e,f], Aleksandra Strogova[a], Kseniya Sirotsina[a], Hanna Yurlevich[a], Darya Novik[a]

[a]*Belarusian State University, ISEI BSU, Minsk, Republic of Belarus*
[b]*Institute of Physical Organic Chemistry, National Academy of Sciences of Belarus,13 Surganov Str., Minsk 220072*
[c]*Institute of Chemistry of New Materials, National Academy of Sciences of Belarus, 36 Skarina Str., Minsk 220141*
[d]*Young Researchers and Elite Club, Gorgan Branch, Islamic Azad University, Gorgan, Iran*
[e]*Department of Chemistry, Faculty of Science, University of Benghazi, Benghazi, Libya*
[f]*Departmentof Chemistry, University of Cape Town, Rondebosch 7701, South Africa*

Abstract

In this research, the four new pyrimidine derivatives have been studied by using density functional theory (DFT/B3LYP/6-31G*) in solvent water for the first time. After quantum-chemical calculations, the title compounds have been synthesized. The electronic spectra of the new derivatives in a solvent water were performed by temporally dependent density functional theory (TD-DFT) method. The equilibrium geometry, the HOMO and LUMO orbitals, MEP, excitation energies, natural charges, oscillator strengths for the molecules have also been calculated. NBO analysis has been calculated in order to elucidate the intramolecular, rehybridization and delocalization of electron density. These molecules have high antioxidant potential due to the planarity and formation of intramolecular hydrogen bonds. Antioxidant properties of the title compound have been investigated and discussed.

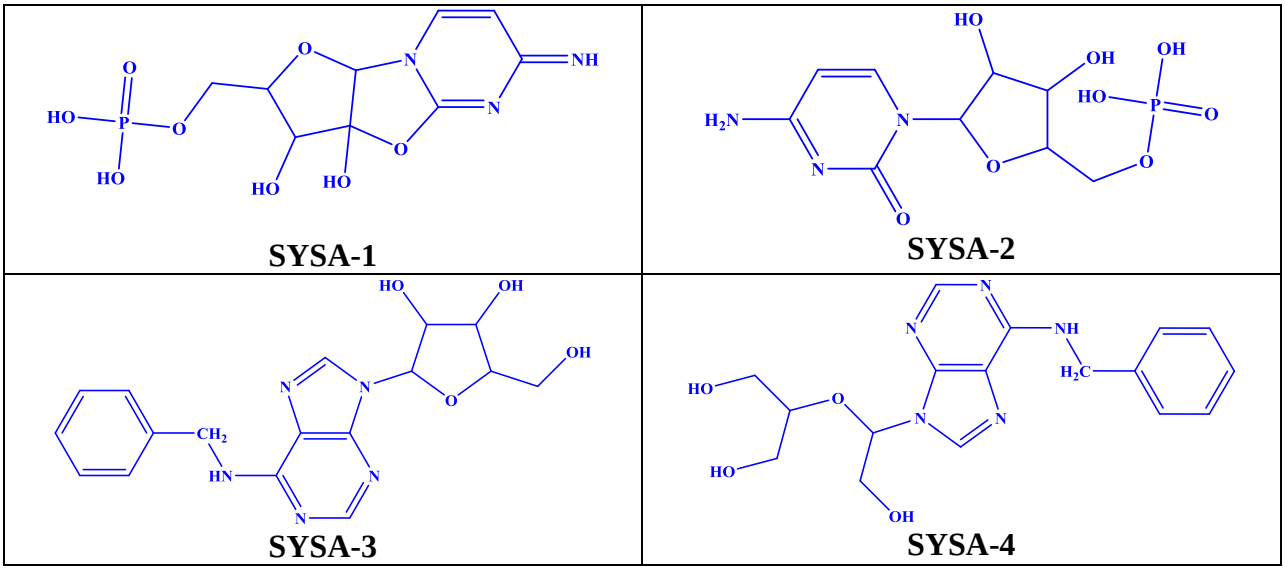

Keywords: pyrimidine; UV/Vis spectrum; NBO; DFT; antioxidant activity; natural charge

Corresponding authors: siyamak.shahab@yahoo.com & m.sheikhi2@gmail.com

1. Introduction

Heterocycles are usually present in most drug molecules because they possess hydrogen bond donors and acceptors and can interact with target enzymes and receptors via hydrogen bond interactions. Heterocycles can modulate lipophilicity of the drugs or improve aqueous solubility of the molecules, thus providing desired pharmacokinetic and pharmaceutical properties [1-3]. Heterocycles containing pyrimidine ring are interest compounds because they constitute an important class of natural and nonnatural products [4,5]. Pyrimidine nuclei have been a source of great interest to organic, medicinal, and material scientists over many years and there has been considerable interest in the development of preparative methods for the production of pyrimidines. The pyrimidine derivatives have been used as histamine and adenosine receptor antagonists as well as among several other biological receptors and modulators [6]. These products show a broad spectrum of biological activities including antioxidante [7] diuretic [8], antitumor [9], anti-HIV [10], cardiovascular [11], analgesic [12], calcium antagonist [13], anti inflammatory [14], CNS depressant activity [15], and antimalarial activity [16].

Experimental works are helpful in describing the antioxidant activity of molecular structure, but they are usully costly and time consuming. With the development of chemistry softwar, computational chemistry and quantum calculations have been a significant tool for chemist to interpret various chemical properties and phenomena, chemical reactions [17], especially catalysis [18], structural determination of organic compounds [19], prediction of spectroscopic data such as ^{1}H NMR and ^{13}C NMR chemical shifts [20], IR, UV/Vis and calculation of properties of the organic molecules [21]. Time-Dependent Density Functional Theory (TD-DFT) is used for predicting the absorption spectrum of the molecules [22-24]**.** We have recently synthesized a series of new azomethine and anthraquinone derivatives and have studied their antioxidant activity and the charge distributions using quantum-chemical calculations and interpreted the free radical scavenging capacity of the investigated structures and their radicals [25,26].

In current study, we reported the synthesis, antioxidant property and equilibrium geometries of the four new pyrimidine derivatives. The parameters like natural Charges, NBO analysis, Ionization Potential (I) and Electron Affinities (A), HOMO and LUMO energies, Hardness (η),

Softness (S), Electronegativity (μ), Electrophilic Index (ω), Electron Donating Power (ω^-), Electron Accepting Power (ω^+) and Energy Gap (E_g) have been calculated for investigated compounds by B3LYP method with 6-31G* basis set. We also were reported the results of DFT calculations to investigate absorption spectrum, UV/Vis, FMO and MEP of four new pyrimidine derivatives.

2. Computational details

The quantum chemical calculations were carried out for the optimization of the new pyrimidine derivatives (**SYSA-1,2,3,4**) using the Gaussian 09W software programs [27] on a Pentium IV/4.28 GHz personal computer using functional B3LYP with 6-31G* basis set in the solvent water. Without any constraint on the geometry, the energies of the title molecules were minimized, completely intramolecular forces were brought to be zero. The IEFPCM (Integral Equation Formalism Polarized Continuum Model) [28] was used for calculations of the solvent effect. The electronic transitions of new derivatives were calculated using TD-DFT method. The theoretical absorption spectrum of the compunds in the solvent water was calculated using TDB3LYP/6-31G* method. The electronic properties such as dipole moment (μ_D), point group, E_{HOMO}, E_{LUMO}, HOMO-LUMO energy gap and natural charges [29] were computed. The optimized molecular structures, MEP, HOMO and LUMO surfaces were visualized using GaussView 05 program [30]. The electronic structure of the title compounds was studied by using Natural Bond Orbital (NBO) analysis [31] at the B3LYP/6-31G* level of theory in order to computed hyperconjugative interactions and charge delocalization.

3. Results and Discussion

3.1 Optimized Structure of the Compounds SYSA-1,2,3,4

The four structures (**SYSA-1,2,3,4**) have optimized using B3LYP/6-31G* level of theory. The calculations were carried out in the solvent water using the IEFPCM (Integral Equation Formalism PCM) method coupled to UAKS radii. The Integral Equation Formalism PCM, by Cances, Mennucci and Tomasi is the most popular PCM version. The optimized structures and parameters are shown in Fig. 1 and Tables 1,2,3,4.

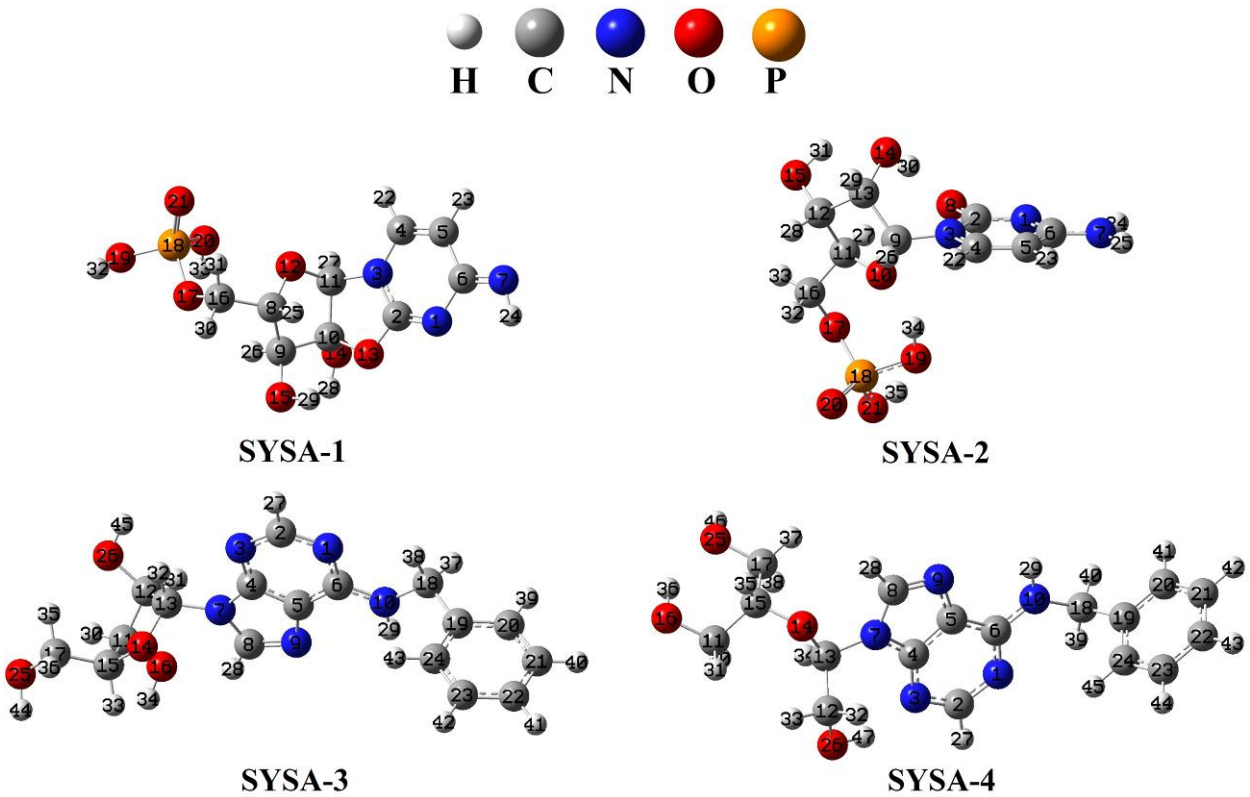

Fig. 1 Optimized molecular structures of the molecules **SYSA-1,2,3,4** calculated by B3LYP/6-31G* level of theory

Table 1 Selected optimized geometrical parameters (Bond lengths (Å) and Bond angles (°)) of the compound **SYSA-1** calculated by B3LYP/6-31G* level of theory.

Parameter	Bond lengths (Å)		Parameter	Bond angles (°)	
	Experimental	Calculated		Experimental	Calculated
N1-C2	1.286	1.281	N1-C2-N3	127.36	127.39
N1-C6	1.418	1.415	N1-C6-C5	117.60	117.59
C2-N3	1.377	1.370	N1-C6-N7	122.20	122.16
N3-C4	1.388	1.388	C2-N1-C6	117.21	117.18
C4-C5	1.350	1.346	C2-N3-C4	118.30	118.31
C5-C6	1.468	1.468	N3-C4-C5	118.72	118.70
C6-N7	1.292	1.290	C4-C5-C6	120.75	120.79
C8-C9	1.543	1.541	C5-C6-N7	120.25	120.23
C2-O13	1.354	1.354	C2-N3-C11	112.35	112.33
N3-C11	1.454	1.450	N3-C2-O13	110.03	110.05
N7-H24	1.023	1.025	N3-C4-H22	116.31	116.32
C8-O12	1.442	1.440	C8-C9-C10	101.95	101.99
C8-C16	1.517	1.516	C8-C9-O15	115.82	115.81
C8-H25	1.101	1.100	C9-C8-C16	115.70	115.70
C9-C10	1.543	1.541	C6-N7-H24	108.28	108.27
C9-O15	1.408	1.404	N3-C11-H27	111.53	111.49
C10-C11	1.545	1.548	C8-O12-C11	109.71	109.73
C10-O13	1.462	1.464	C2-O13-C10	109.59	109.61
C10-O14	1.377	1.374	N3-C11-C10	101.50	101.49
C11-O12	1.413	1.414	C9-C10-O14	117.29	117.30

C16-O17	1.444	1.444	O12-C8-C16	109.04	109.02
O17-P18	1.614	1.613	C8-C16-O17	111.90	111.92
P18-O19	1.612	1.610	O13-C10-O14	110.40	110.39
P18-O20	1.600	1.603	C16-O17-P18	121.88	121.87
P18-O21	1.477	1.479	O17-P18-O19	100.84	100.86
C11-H27	1.092	1.090	O17-P18-O20	108.03	108.03
O14-H28	0.971	0.974	O17-P18-O21	115.30	115.31
O15-H29	0.972	0.973	O19-P18-O20	100.63	100.66
C16-H30	1.092	1.092	C19-P18-O21	118.19	118.21
C16-H31	1.095	1.092	O20-P18-O21	112.12	112.13
O19-H32	0.974	0.973	P18-O19-H32	112.54	112.57
O20-H33	0.974	0.973	P18-O20-H33	113.70	113.73

Table 2 Selected optimized geometrical parameters (Bond lengths (Å) and Bond angles (°)) of the compound **SYSA-2** calculated by B3LYP/6-31G* level of theory.

Parameter	Bond lengths (Å)		Parameter	Bond angles (°)	
	Experimental	Calculated		Experimental	Calculated
N1-C2	1.350	1.348	N1-C2-N3	118.95	118.96
N1-C6	1.336	1.335	N1-C2-O8	122.45	122.41
C2-N3	1.427	1.424	N1-C6-C5	122.41	122.37
C2-O8	1.245	1.248	N1-C6-N7	117.40	117.51
N3-C4	1.370	1.372	C2-N1-C6	120.56	120.59
C4-C5	1.355	1.354	C2-N3-C4	119.75	119.71
C5-C6	1.433	1.433	N3-C4-C5	121.69	121.63
C6-N7	1.340	1.342	C4-C5-C6	116.63	116.65
N3-C9	1.470	1.469	C5-C6-N7	120.11	120.11
C5-H23	1.078	1.082	N3-C2-O8	118.65	118.61
N7-H24	1.011	1.010	N3-C4-H22	116.20	116.17
N7-H25	1.008	1.009	N3-C9-C13	117.80	117.78
C9-O10	1.433	1.433	N3-C9-O10	110.55	110.54
C9-C13	1.550	1.552	C9-O10-C11	110.89	110.89
C9-H26	1.093	1.091	C9-C13-O14	116.75	116.76
C10-C11	1.448	1.448	C9-C13-C12	102.17	102.16
C11-C12	1.540	1.539	O10-C9-C13	106.90	106.89
C12-C13	1.555	1.553	O10-C11-C12	103.65	103.65
C12-O15	1.401	1.405	C11-C12-C13	102.19	102.18
C13-O14	1.413	1.412	C11-C12-O15	114.29	114.23
C11-C16	1.519	1.514	C12-C13-O14	109.96	109.93
C16-O17	1.449	1.447	O10-C11-C16	109.21	109.27
O17-P18	1.609	1.618	C11-C16-O17	111.31	111.71
P18-O19	1.603	1.605	C16-O17-P18	120.61	120.65
P18-O20	1.480	1.482	O17-P18-O19	105.55	105.59
P18-O21	1.604	1.602	O17-P18-O20	114.81	114.81
C11-H27	1.099	1.095	O17-P18-O21	102.44	102.41
C12-H28	1.098	1.096	O19-P18-O20	117.15	117.13
O14-H30	0.992	0.991	C19-P18-O21	102.64	102.61
O15-H31	0.980	0.979	O20-P18-O21	112.57	112.56
O19-H34	0.985	0.989	P18-O19-H34	109.89	109.87

O21-H35		0.973	P18-O21-H35	113.30	113.30

Table 3 Selected optimized geometrical parameters (Bond lengths (Å) and Bond angles (°)) of the compound **SYSA-3** calculated by B3LYP/6-31G* level of theory.

Parameter	Bond lengths (Å)		Parameter	Bond angles (°)	
	Experimental	Calculated		Experimental	Calculated
N1-C2	1.346	1.343	N1-C2-N3	128.99	128.94
N1-C6	1.354	1.350	N1-C6-C5	118.30	118.23
C2-N3	1.334	1.335	C2-N1-C6	118.50	118.55
N3-C4	1.343	1.343	C2-N3-C4	111.29	111.25
C4-C5	1.396	1.395	N3-C4-C5	126.66	126.60
C4-N7	1.381	1.382	N3-C4-N7	128.20	128.15
C5-C6	1.419	1.415	C4-C5-C6	116.43	116.39
C5-N9	1.380	1.385	C4-C5-N9	111.19	111.10
N7-C8	1.386	1.383	C4-N7-C8	105.93	105.91
C8-N9	1.316	1.314	C5-N9-C8	104.15	104.12
C2-H27	1.089	1.088	N7-C8-N9	113.60	113.61
C6-N10	1.353	1.353	C4-N7-C13	125.35	125.32
N7-C13	1.457	1.459	C5-C6-N10	121.28	121.28
N10-C18	1.455	1.456	C8-N7-C13	128.68	128.64
N10-H29	1.012	1.011	C6-N10-C18	125.47	125.46
C11-C12	1.534	1.534	N7-C13-C12	114.83	114.80
C11-C15	1.539	1.536	N10-C18-C19	112.85	112.81
C11-O16	1.422	1.426	C11-C12-C13	103.59	103.58
C12-C13	1.555	1.554	C11-C15-O14	106.16	106.10
C12-O26	1.424	1.420	C11-C15-C17	113.80	113.79
C13-O14	1.421	1.419	C12-C13-O14	107.10	107.04
O14-C15	1.440	1.442	C13-C12-O26	111.05	111.03
C15-C17	1.533	1.534	C13-O14-C15	111.39	111.36
C17-O25	1.425	1.423	O14-C15-C17	109.43	109.41
C18-C19	1.518	1.518	C15-C17-O25	111.71	111.69
C19-C20	1.400	1.399	C18-C19-C20	120.27	120.23
C19-C24	1.405	1.402	C18-C19-C24	120.90	120.92
C20-C21	1.399	1.397	C19-C20-C21	120.74	120.71
C21-C22	1.394	1.395	C19-C24-C23	120.62	120.59
C22-C23	1.399	1.398	C20-C21-C22	120.07	120.06
C23-C24	1.397	1.395	C21-C22-C23	119.61	119.61
O25-H44	0.971	0.970	C22-C23-C24	120.19	120.18

Table 4 Selected optimized geometrical parameters (Bond lengths (Å) and Bond angles (°)) of the compound **SYSA-4** calculated by B3LYP/6-31G* level of theory.

Parameter	Bond lengths (Å)		Parameter	Bond angles (°)	
	Experimental	Calculated		Experimental	Calculated
N1-C2	1.339	1.338	N1-C2-N3	128.55	128.50
N1-C6	1.351	1.351	N1-C6-C5	118.31	118.31
C2-N3	1.338	1.336	C2-N1-C6	118.69	118.68
N3-C4	1.343	1.348	C2-N3-C4	112.10	112.11

C4-C5	1.397	1.395	N3-C4-C5	125.70	125.68
C4-N7	1.386	1.380	N3-C4-N7	128.74	128.77
C5-C6	1.420	1.417	C4-C5-C6	116.69	116.68
C5-N9	1.385	1.381	C4-C5-N9	111.10	111.06
N7-C8	1.386	1.383	C4-N7-C8	105.55	105.52
C8-N9	1.317	1.314	C5-N9-C8	103.96	103.95
C2-H27	1.089	1.087	N7-C8-N9	113.95	113.91
C6-N10	1.350	1.349	C4-N7-C13	127.85	127.85
N7-C13	1.486	1.485	C5-C6-N10	121.20	121.21
N10-C18	1.461	1.461	C8-N7-C13	126.54	126.57
N10-H29	1.015	1.012	C6-N10-C18	125.60	125.60
C11-C15	1.543	1.540	N7-C13-C12	112.08	112.06
C11-O16	1.419	1.419	N7-C13-O14	106.55	106.51
C12-C13	1.546	1.545	N10-C18-C19	113.16	113.17
C12-O26	1.411	1.410	C11-C15-O14	112.56	112.56
C13-O14	1.409	1.409	C11-C15-C17	113.53	113.49
O14-C15	1.442	1.441	C12-C13-O14	110.44	110.39
C15-C17	1.539	1.535	C13-C12-O26	113.09	113.05
C17-O25	1.436	1.432	C13-O14-C15	118.82	118.79
C18-C19	1.518	1.518	O14-C15-C11	112.51	112.56
C19-C20	1.401	1.399	O14-C15-C17	111.10	111.13
C19-C24	1.400	1.403	C15-C11-O16	111.55	111.57
C20-C21	1.399	1.398	C15-C17-O25	107.50	107.51
C21-C22	1.394	1.395	C18-C19-C20	120.61	120.59
C22-C23	1.399	1.398	C19-C20-C21	120.66	120.69
C23-C24	1.395	1.394	C20-C21-C22	120.05	120.02
O25-H46	0.970	0.969	C21-C22-C23	119.64	119.68
O26-H47	0.985	0.987	C22-C23-C24	120.18	120.14

3.2. FMO Analysis and Electronic Properties of the Compounds SYSA-1,2,3,4

The frontier molecule orbitals (FMOs) are including HOMO and the LUMO orbitals that participate in electronic properties, optical properties, UV/Vis spectrum and chemical reactions [28]. We calculated the energies of HOMO and the LUMO orbitals and the electronic properties of compounds **SYSA-1,2,3,4** using B3LYP/6-31G* level of theory. The calculated results are summarized in Table 5.

Table 5 The calculated electronic properties of the compounds **SYSA-1,2,3,4** using B3LYP/6-31G* level of theory.

Property	SYSA-1	SYSA-2	SYSA-3	SYSA-4
HF (Hartree)	-1457.645	-1458.896	-1233.897	-1235.097
Dipole moment (Debye)	9.288	12.018	3.699	6.250
Point Group	C1	C1	C1	C1
E_{HOMO} (eV)	-6.06	-6.72	-5.87	-5.99
E_{LUMO} (eV)	-0.69	-1.18	-0.64	-0.82
Eg (eV)	5.37	5.54	5.23	5.17
I (eV)	6.06	6.72	5.87	5.99
A (eV)	0.69	1.18	0.64	0.82

χ (eV)	3.37	3.95	3.25	3.40
η (eV)	2.68	2.77	2.61	2.58
μ (eV)	-3.37	-3.95	-3.25	-3.40
ω (eV)	2.11	2.81	2.02	2.24
ω^+ (eV)	0.189	0.231	0.186	0.204
ω^- (eV)	0.439	0.481	0.436	0.454
S (eV)	0.186	0.180	0.191	0.193

The image of calculated HOMO and LUMO orbitals of the title compounds is shown in Fig. 2. The positive and negative phases are in red and green colors, respectively. As shown in Fig. 2, the HOMO and LUMO orbitals of compound **SYSA-1** are mainly focused on double bond (-C=C- and -C=N-) of the pyrimidine ring and nitrogen atom of imine group. The electron density of HOMO orbital of molecule **SYSA-2** is mainly focused on double bonds (-C=C- and -C=N-) of the pyrimidine ring, nitrogen atom of amine group, oxygen atoms of carbonyl group, tetrahydrofuran and hydroxyl groups of on tetrahydrofuran ring, whereas the LUMO orbital is localized on pyrimidine ring and nitrogen atom of amine group. The HOMO orbital of compound **SYSA-3** are mainly focused on double bond (-C=C-) of the phenyl ring, while the LUMO orbital is localized on double bonds (-C=C- and -C=N-) of the purine ring and nitrogen atom of the amine group. The HOMO orbital of compound **SYSA-4** are mainly focused on double bond (-C=C-) of the phenyl ring and partially on the pyrimidine ring and nitrogen atom of the amine group, whereas the LUMO orbital is localized on double bonds (-C=C- and -C=N-) of the purine ring and nitrogen atom of the amine group (Fig. 2). Thus, the most of the charge transfer from the HOMO to LUMO in compounds **SYSA-1,2,3,4** takes place due to the contribution of pi (π) bonds and lone pairs.

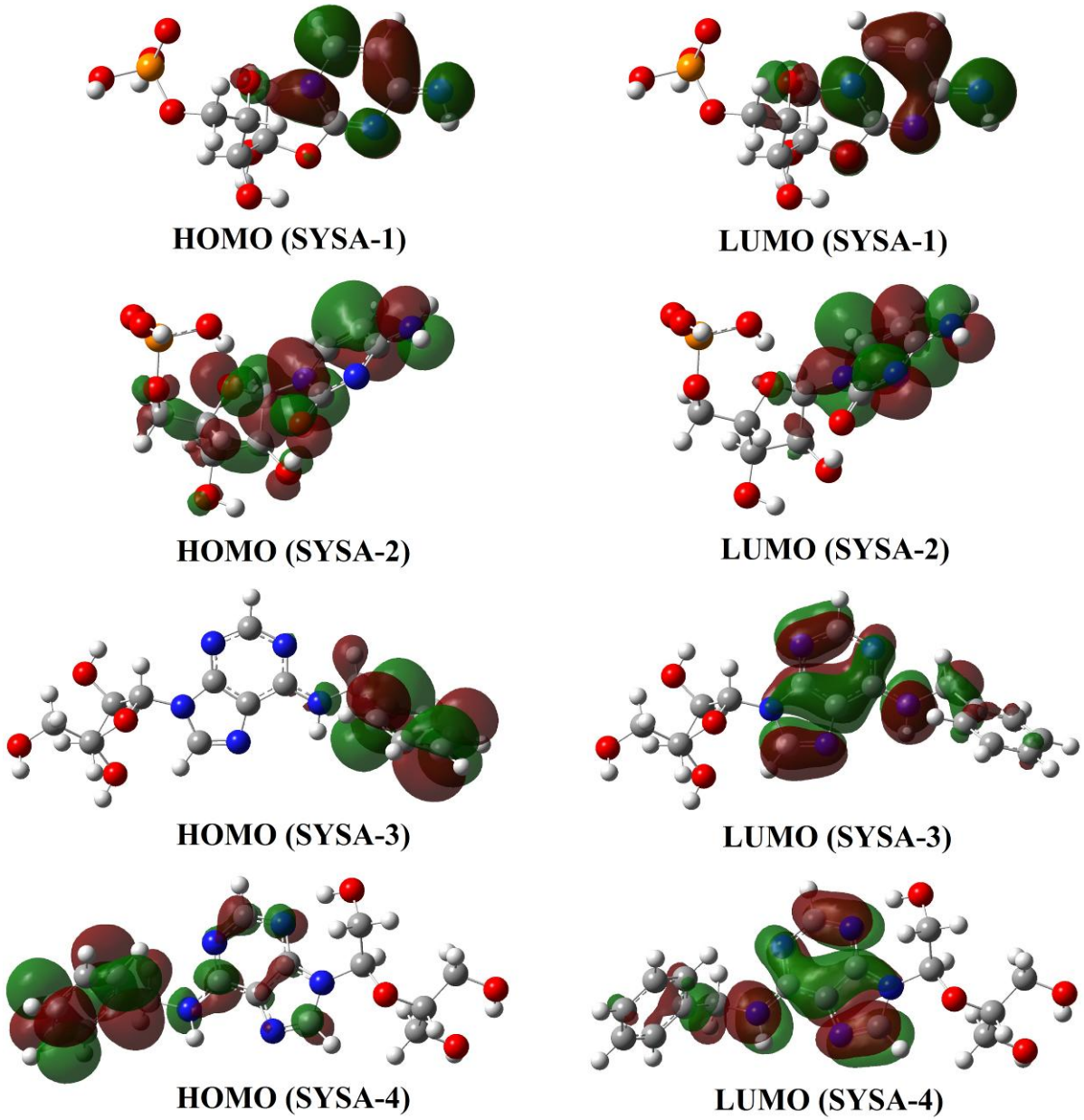

Fig. 2 Calculated HOMO and LUMO orbitals of compounds **SYSA-1,2,3,4** by B3LYP/6-31G* level of theory.

The energy of HOMO orbital (E_{HOMO}) and the energy of LUMO orbital (E_{LUMO}) are related to the ionization potential (I=-E_{HOMO}) and the electron affinity (A=-E_{LUMO}), respectively [25]. The global hardness (η), electronegativity (χ), electronic chemical potential (μ) and electrophilicity (ω), electron donating power (ω^-= *(3I+A)2/16(I-A)*), electron accepting power (ω^+= *(I+3A)2/16(I-A)*) and chemical softness (S) parameters [26] are calculated with the following equations:

(η=*I-A*/2) (1)

(χ=*I*+*A*/2) (2)

(μ=-(*I*+*A*)/2) (3)

(ω=μ^2/2η) (4)

ω^+= *(I+3A)2/16(I-A)* (5)

ω^-= *(3I+A)2/16(I-A)* (6)

(*S*=*1/2*η) (7)

in which values of these parameters are reported in Table 5. The global hardness (η) parameter is related to the energy gap (Eg = $E_{LUMO} - E_{HOMO}$) and defined as measurement from the resistance of an atom or a group of atoms to charge transfer [].

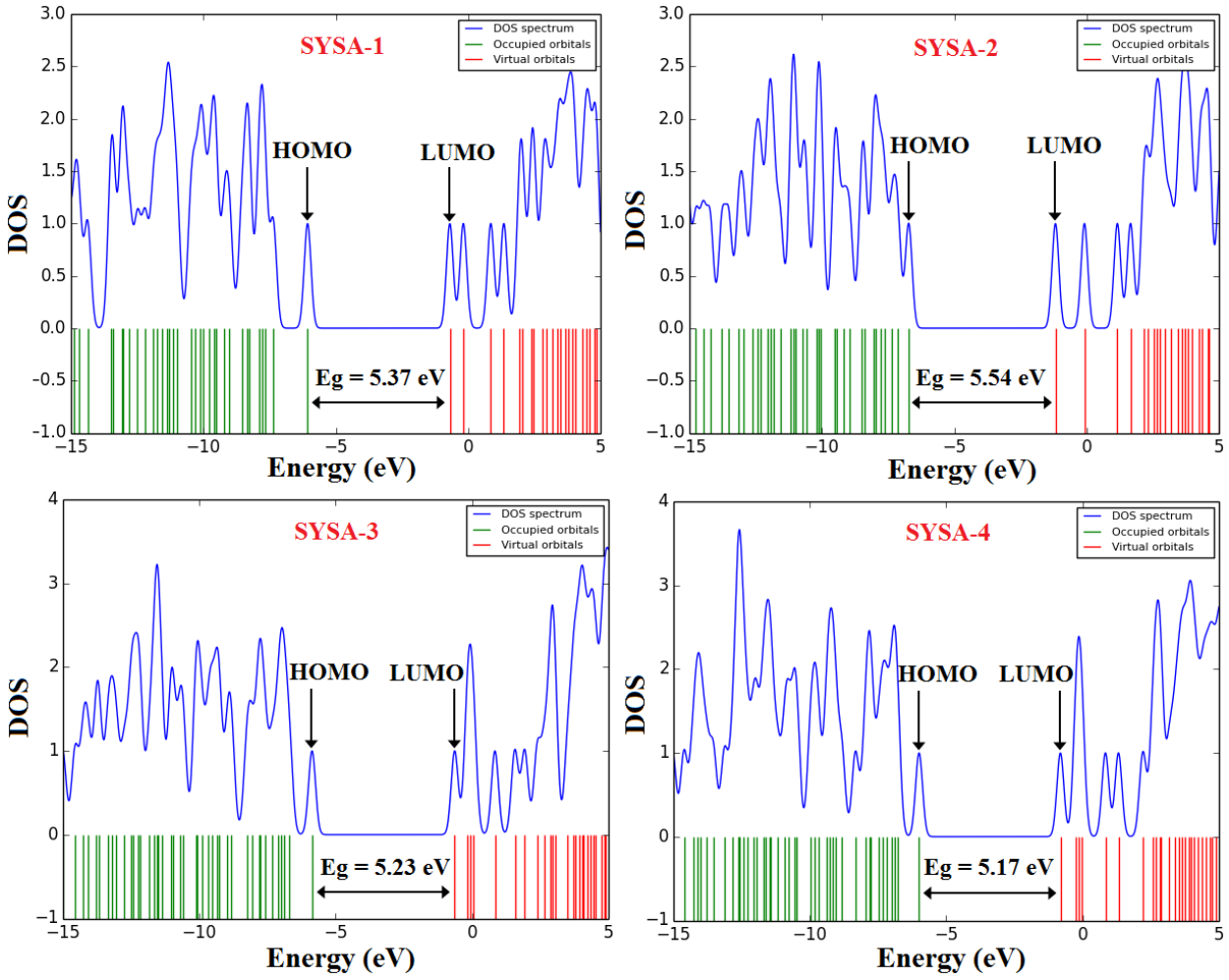

Fig. 3 DOS plots of compounds **SYSA-1,2,3,4** by B3LYP/6-31G* level of theory.

The Eg is an important parametre determining molecular electrical transport properties and reactivity of the molecules [23]. The electronic transport at the molecule with a low gap is

simpler. A molecule with a low Eg has a high chemical reactivity, low kinetic stability and is a soft molecule; whereas a hard molecule has a large Eg [26]. The calculated energy gap of the compounds **SYSA-1, SYSA-2, SYSA-3, SYSA-4** was estimated about 5.37 eV, 5.54 eV, 5.23 eV and 5.17 eV, respectively. Total electronic densities of states (DOSs) plots [32] in Fig. 3 also show the energy gaps of the title compounds. The global hardness of compounds **SYSA-1, SYSA-2, SYSA-3, SYSA-4** is 2.68 eV, 2.77 eV, 2.61 eV and 2.58 eV, respectively. The energy gap (Eg) and global hardness (η) of title compounds can be ranged in the following sequence: **SYSA-2**>**SYSA-1**>**SYSA-3**>**SYSA-4**. The chemical softness (*S*) index describes the capacity of an atom or a group of atoms to receive electrons [26]. The chemical softness (*S*) of title compounds can be ranged in the following sequence: **SYSA-4**>**SYSA-3**>**SYSA-1**>**SYSA-2**. Therefore, the molecule **SYSA-4** is the softer compound compared with other compounds. Electronegativity (χ) parameter is a measure of the power of an atom or a group of atoms to attract electrons [25]. The ionization potential shows the facility of the electron donating of the investigated compounds due to electron abstraction is the first antioxidant mechanism. Therefore, compounds with low ionization potential values can easily undergo oxidation. Antioxidant activity of title compounds can be ranged in the following sequence: **SYSA-2**>**SYSA-1**>**SYSA-4**>**SYSA-3**. The compound **SYSA-3** has the lowest electron affinity (*A*) value (0.64 eV) comparing with other neutral azomethines. The Electrophilic Index (ω) represents the stabilization energy of the molecular systems when electrons saturate it [26]. The results show that **SYSA-3** has the lowest value ω (2.02 eV) and is nucleophilic, whereas **SYSA-2** has the highest value ω (2.81 eV) and is strongly electrophilic. In addition, the radical **SYSA-2** has the highest electron accepting power (ω^+ = 0.231 eV) and electron donating power (ω^- = 0.481 eV) values.

3.3. MEP Analysis of the Compounds A and B

MEP maps show the electronic density and are used in determination of the negative and positive electrostatic potentials regions of the molecular structure for electrophilic attacks and nucleophilic reactions [33]. The difference of the electrostatic potential at the surface is shown by different colors. The regions of electron rich, partially negative charge, slightly electron rich sites, positive charge or electron poor and neutral sites in the MEP maps are red, orange, yellow, blue, and green colors, respectively [34]. The MEP surfaces of molecules **SYSA-1,2,3,4** were calculated by theoretical calculations using the B3LYP/6-31G* level of theory (Fig. 4). As we

can see from the Fig. 4, the negative site (red color) of molecule **SYSA-1** is mostly focused on nitrogen atom of imine group (N7). In addition, the O21 atom with yellow color is slightly electron rich site and the H28, H29, H32, H33 atoms in the hydroxyl groups of **SYSA-1** show regions with positive charges. The oxygen atoms of carbonyl groups (O8 and O20) of **SYSA-2** have red color that is shown electron rich sites, whereas the H24, H25 atoms in the amine group and H35 atom in the hydroxyl group with blue color are shown electron poor sites. In the molecule **SYSA-3**, the N1, N3, N9 atoms of purine ring and phenyl ring with yellow color are shown slightly electron rich sites and the H34, H44, H45 atoms with blue color are electron poor sites. The partially negative charge (orange color) of molecule **SYSA-4** is focused on oxygen atoms of hydroxyl groups (O16 and O26 atoms) and the H46 atom in the hydroxyl group show region with positive charges. The regions with green color in the molecules **SYSA-1,2,3,4** show sites with zero potential and neutral regions.

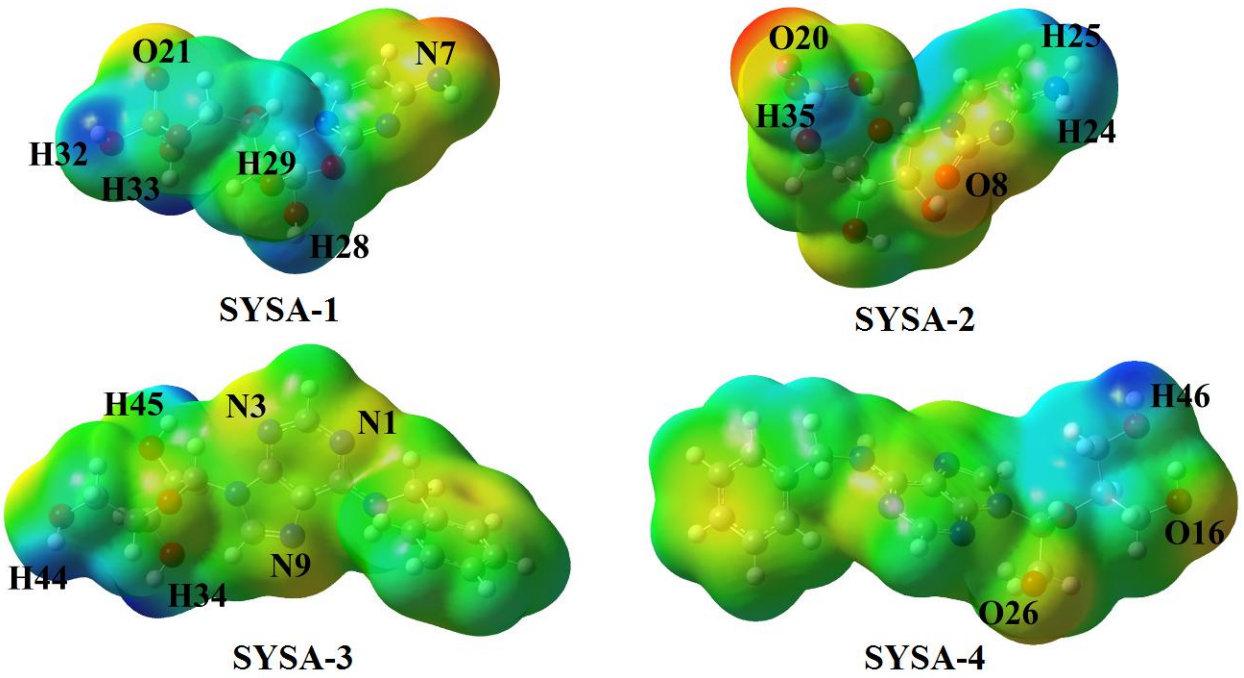

Fig. 4 MEP maps of the molecules **SYSA-1,2,3,4** calculated using the B3LYP/6-31G* level of theory.

3.4. Natural Charge Analysis of the Compounds SYSA-1,2,3,4

The atomic charges play a significant role in molecules because the atomic charges affect electronic structure, dipole moment, polarizability, vibrational spectra and other properties of molecular structures []. The atomic charges of molecules **SYSA-1,2,3,4** by NBO analysis using

the B3LYP/6-31G* level of theory in a solvent water were calculated and the results are presented in Table 6 (atoms numbering are according to Fig. 1). The total charge of compounds **SYSA-1,2,3,4** is equal to zero. The NBO analysis of the title compounds shows that carbon atoms have both positive and negative charges. As shown in Table 6, the positive carbons are observed for the carbon atoms attachment to the electron-withdrawing oxygen and nitrogen atoms including C2 (0.783e), C4 (0.017e), C6 (0.380e), C8 (0.025e), C9 (0.034e), C10 (0.544e), C11 (0.248e) atoms in compounds **SYSA-1**, C2 (0.818e), C4 (0.080e), C6 (0.459e), C9 (0.249e), C11 (0.028e), C12 (0.053e), C13 (0.041e) atoms in compound **SYSA-2**, C2 (0.253e), C4 (0.370e), C5 (0.002e), C6 (0.438e), C8 (0.230e), C11 (0.052e), C12 (0.055e), C13 (0.242e), C15 (0.031e) atoms in compound **SYSA-3**, C2 (0.272e), C4 (0.338e), C5 (0.010e), C6 (0.442e), C8 (0.231e), C13 (0.257e), C15 (0.041e) atoms in compound **SYSA-4**. The C2 atom of pyrimidine ring at the compounds **SYSA-1** and **SYSA-2** ((0.783e) and (0.818e), respectively) and the C6 atom of purine ring at the compounds **SYSA-3 and SYSA-4** ((0.438e) and (0.442e), respectively) have the more positive charge comparing with other carbon atoms due to the attachment to two electron-withdrawing nitrogens. According to the calculations, all hydrogen atoms of the title compounds (SYSA-1,2,3,4) have the positive charge and the hydrogen atoms attached to oxygen and nitrogen atoms has the highest positive charge comparing with other atoms. The P18 atom in molecules **SYSA-1** and **SYSA-2** has the highest positive charge rather than other atoms.

Table 6 NBO charges (e) of the compounds **SYSA-1,2,3,4** calculated using the B3LYP/6-31G* level of theory.

SYSA-1		SYSA-2		SYSA-3		SYSA-4	
Atoms	Charge	Atoms	Charge	Atoms	Charge	Atoms	Charge
N1	-0.586	N1	-0.613	N1	-0.588	N1	-0.583
C2	0.783	C2	0.818	C2	0.253	C2	0.272
N3	-0.476	N3	-0.467	N3	-0.564	N3	-0.598
C4	0.017	C4	0.080	C4	0.370	C4	0.368
C5	-0.317	C5	-0.369	C5	0.002	C5	0.010
C6	0.380	C6	0.459	C6	0.438	C6	0.442
N7	-0.743	N7	-0.776	N7	-0.430	N7	-0.429
C8	0.025	O8	-0.721	C8	0.230	C8	0.231
C9	0.034	C9	0.249	N9	-0.518	N9	-0.517
C10	0.544	O10	-0.623	N10	-0.598	N10	-0.588
C11	0.248	C11	0.028	C11	0.052	C11	-0.133
O12	-0.587	C12	0.053	C12	0.055	C12	-0.126
O13	-0.556	C13	0.041	C13	0.242	C13	0.257
O14	-0.734	O14	-0.792	O14	-0.593	O14	-0.595
O15	-0.749	O15	-0.765	C15	0.031	C15	0.041
C16	-0.119	C16	-0.126	O16	-0.776	O16	-0.782
O17	-0.866	O17	-0.861	C17	-0.122	C17	-0.127
P18	2.571	P18	2.566	C18	-0.271	C18	-0.273
O19	-1.021	O19	-1.042	C19	-0.060	C19	-0.062

O20	-0.019	O20	-1.106	C20	-0.234	C20	-0.233
O21	-1.101	O21	-1.021	C21	-0.235	C21	-0.235
H22	0.265	H22	0.262	C22	-0.243	C22	-0.241
H23	0.265	H23	0.271	C23	-0.235	C23	-0.235
H24	0.356	H24	0.438	C24	-0.231	C24	-0.228
H25	0.246	H25	0.439	O25	-0.770	O25	-0.781
H26	0.264	H26	0.261	O26	-0.766	O26	-0.795
H27	0.277	H27	0.248	H27	0.219	H27	0.225
H28	0.512	H28	0.242	H28	0.250	H28	0.247
H29	0.498	H29	0.257	H29	0.436	H29	0.438
H30	0.255	H30	0.505	H30	0.247	H30	0.197
H31	0.251	H31	0.493	H31	0.246	H31	0.226
H32	0.540	H32	0.237	H32	0.257	H32	0.209
H33	0.540	H33	0.256	H33	0.239	H33	0.232
		H34	0.535	H34	0.501	H34	0.234
		H35	0.540	H35	0.228	H35	0.252
				H36	0.214	H36	0.498
				H37	0.241	H37	0.218
				H38	0.270	H38	0.212
				H39	0.242	H39	0.268
				H40	0.244	H40	0.248
				H41	0.244	H41	0.242
				H42	0.244	H42	0.245
				H43	0.244	H43	0.244
				H44	0.488	H44	0.245
				H45	0.501	H45	0.244
						H46	0.511
						H47	0.500

3.5. NBO Analysisof the Compound SYSA-2

NBO analysis is a good method of studying intra- and inter-molecular bonding and interaction between bonds and charge transfer in molecular structure [26]. The filled NBOs and empty filled NBOs and the stabilization energy ($E^{(2)}$) calculated from the second-order micro disturbance theory of the compound **SYSA-2** are summarized in Table 7.

Table 7 Significant donor–acceptor interactions and second order perturbation energies of the compound **SYSA-2** calculated using the B3LYP/6-31G* level of theory.

Donor (i)	Occupancy	Acceptor (j)	Occupancy	$E^{(2)a}$ kcal/mol	E(j)-E(i)[b] a.u.	F(i , j)[c] a.u.
π(N1-C6)	1.75172	π*(N1-C6)	0.44516	3.39	0.30	0.030
		π*(C2-O8)	0.45062	42.93	0.30	0.106
		π*(C4-C5)	0.20216	5.92	0.33	0.040
π(C4-C5)	1.81528	π*(N1-C6)	0.44516	25.49	0.28	0.081
		π*(C4-C5)	0.20216	2.85	0.30	0.026
π*(N1-C6)	0.11516	π*(C4-C5)	0.20216	108.77	0.02	0.079
σ(C4-H22)	1.98033	σ*(C2-N3)	0.10809	4.54	0.93	0.059
σ(C5-H23)	1.97610	σ*(N1-C6)	0.02199	4.28	1.07	0.060
		σ*(N3-C4)	0.02397	5.61	0.99	0.066
σ(N7-H24)	1.98988	σ*(C5-C6)	0.03625	4.57	1.16	0.066
σ(N7-H25)	1.99003	σ*(N1-C6)	0.02199	4.69	1.20	0.067
σ(O10-C11)	1.98595	σ*(C12-O15)	0.01653	1.72	1.13	0.039
		σ*(C16-H33)	0.01519	1.04	1.27	0.032

σ(O17-P18)	1.97198	σ*(C16-H33)	0.01519	1.06	1.26	0.033
		σ*(P18-O19)	0.18888	3.74	1.04	0.058
		σ*(P18-O20)	0.10054	2.25	1.17	0.047
		σ*(P18-O21)	0.15855	3.87	1.04	0.059
σ(P18-O19)	1.97727	σ*(O17-P18)	0.20042	3.66	1.05	0.058
		σ*(P18-O19)	0.18888	0.52	1.06	0.022
		σ*(P18-O20)	0.10054	2.07	1.18	0.045
		σ*(P18-O21)	0.15855	4.54	1.05	0.064
n1(N1)	1.89413	σ*(C2-N3)	0.10809	15.34	0.71	0.093
		σ*(C2-O8)	0.02474	3.76	0.88	0.053
		σ*(C5-C6)	0.03625	11.47	0.83	0.089
		σ*(C6-N7)	0.02937	3.90	0.84	0.052
		σ*(N7-H24)	0.00914	0.53	0.81	0.019
n1(N3)	1.59591	π*(C2-O8)	0.45062	53.10	0.26	0.107
		π*(C4-C5)	0.20216	41.97	0.29	0.104
		σ*(C9-O10)	0.05017	9.27	0.53	0.069
		σ*(C9-C13)	0.05086	4.96	0.60	0.054
n1(N7)	1.69090	π*(N1-C6)	0.44516	67.40	0.26	0.122
n1(O8)	1.95896	σ*(C2-N3)	0.10809	4.34	1.04	0.061
		σ*(O14-H30)	0.06684	8.19	1.10	0.085
n2(O8)	1.85897	σ*(N1-C2)	0.04687	19.97	0.78	0.114
		σ*(C2-N3)	0.10809	20.53	0.65	0.104
		σ*(O14-H30)	0.06684	12.23	0.71	0.085
n1(O10)	1.94294	σ*(C9-C13)	0.05086	2.53	0.87	0.042
		σ*(C19-H34)	0.04483	9.70	0.96	0.086
n2(O10)	1.91492	σ*(N3-C9)	0.05320	7.69	0.69	0.066
		σ*(O19-H34)	0.04483	8.89	0.79	0.076
n1(O14)	1.97526	σ*(C9-C13)	0.05086	2.65	0.89	0.044
		σ*(C12-C13)	0.05478	1.40	0.90	0.032
		σ*(C13-H29)	0.02036	1.89	1.03	0.039
n2(O14)	1.92119	σ*(C9-C13)	0.05086	5.74	0.64	0.054
		σ*(C12-C13)	0.05478	7.30	0.65	0.062
		σ*(O15-H31)	0.03037	6.27	0.74	0.062
n1(O15)	1.97878	σ*(C12-C13)	0.05478	2.99	0.92	0.047
		σ*(C12-H28)	0.02531	1.13	1.04	0.031
n2(O15)	1.94521	σ*(C11-C12)	0.04834	9.53	0.65	0.070
		σ*(C12-C13)	0.05478	2.94	0.64	0.039
n1(O17)	1.95175	σ*(P18-O20)	0.10054	4.37	0.94	0.058
		σ*(P18-O21)	0.15855	3.43	0.81	0.048
n2(O17)	1.90712	σ*(C11-C16)	0.02920	6.05	0.72	0.060
		σ*(P18-O19)	0.18888	10.74	0.57	0.072
n1(O19)	1.96061	σ*(O17-P18)	0.20042	3.38	0.83	0.049
		σ*(P18-O21)	0.15855	2.77	0.83	0.044
n2(O19)	1.91864	σ*(O17-P18)	0.20042	5.31	0.57	0.050
		σ*(P18-O20)	0.10054	11.00	0.70	0.079
n1(O20)	1.97849	σ*(P18-O19)	0.18888	1.08	0.96	0.030
		σ*(P18-O21)	0.15855	1.05	0.95	0.029
n2(O20)	1.81463	σ*(O17-P18)	0.20042	16.37	0.50	0.081
		σ*(P18-O19)	0.18888	20.04	0.50	0.090
n1(O21)	1.96872	σ*(P18-O19)	0.18888	2.38	0.85	0.042
		σ*(P18-O20)	0.10054	1.58	0.97	0.035
n2(O21)	1.92175	σ*(O17-P18)	0.20042	9.89	0.58	0.070
		σ*(P18-O19)	0.18888	5.59	0.58	0.052

[a] $E^{(2)}$ Energy of hyperconjucative interactions,

[b] Energy difference between donor and acceptor i and j NBO orbitals,

[c] F(i, j) is the Fock matrix element between i and j NBO orbitals.

The electron delocalization from the electron donor orbitals to the electron acceptor orbitals describes a conjugative electron transfer process between orbitals [35]. For each donor orbital (*i*) and acceptor orbital (*j*), the interacting stabilization energy $E^{(2)}$ associated with the delocalization $i \rightarrow j$ is computed [35]:

$$E^{(2)} = \Delta E_{ij} = q_i \frac{F(i,j)^2}{\varepsilon_j - \varepsilon_i} \qquad (8)$$

in which q_i is the electron donor orbital occupancy, ε_j and ε_i are diagonal elements and F(i,j) is the off-diagonal NBO Fock matrix element [35]. The stabilization energy ($E^{(2)}$) show the value of participation of electrons in the resonance between atoms. The greater $E^{(2)}$ value, the most intensive is the interaction between donor and acceptor orbitals, i.e. the more donation tendency from electron donors to electron acceptors and the mostly extent of conjugation of the whole molecular system [23]. Delocalization of electron density between occupied Lewis-type (bond or lone pair) NBO orbitals and formally unoccupied (antibonding or Rydberg) non-Lewis NBO orbitals correspond to a stabilization donor–acceptor interaction [24]. NBO analysis has been carried out for the molecule **SYSA-2** using B3LYP/6-31G* level of theory in order to elucidate the intramolecular, rehybridization and delocalization of electron density within molecule **SYSA-2**. The intramolecular hyperconjugative interactions of the compound **SYSA-2** with weak, moderate and strong intensity such as π→π*, π*→π*, σ→σ*, n→π* and n→σ* transitions are summarized in Table 7. According to results of NBO analysis, the σ(P18-O19) orbital acts as electron donor and the anti-bonding σ*(O17-P18), σ*(P18-O19), σ*(P18-O20), σ*(P18-O21) orbitals participate as electron acceptor with stabilization energies ($E^{(2)}$) about 3.66 kcal/mol, 0.52 kcal/mol, 2.07 kcal/mol, 4.54 kcal/mol, respectively, in which these values show that σ(P18-O19)→σ*(P18-O21) interaction has the highest stabilization energy (4.54 kcal/mol) comparing with σ(P18-O19)→σ*(O17-P18), σ(P18-O19)→σ*(P18-O19), σ(P18-O19)→σ*(P18-O20) interactions in the phosphate group. The σ(C5-H23) orbital in pyrimidine ring also acts as electron donor and the anti-bonding σ*(N1-C6), σ*(N3-C4) orbitals participate as electron acceptor with stabilization energies ($E^{(2)}$) about 4.28 kcal/mol, 5.61 kcal/mol, respectively, in which these values show σ(C5-H23)→σ*(N3-C4) interaction has the high resonance energy (5.61 kcal/mol) comparing with σ(C5-H23)→σ*(N1-C6) interaction. The intramolecular hyperconjugative interactions of the π→π* have the higher resonance energies ($E^{(2)}$) rather than σ→σ* transitions. Aa shown in Table 7, the π→π* transitions in Purine ring that lead to

moderate delocalization that are including π(N1-C6)→π*(N1-C6), π(N1-C6)→π*(C2-O8), π(N1-C6)→π*(C4-C5), π(C4-C5)→π*(N1-C6), π(C4-C5)→π*(C4-C5) with the resonance energies ($E^{(2)}$) 3.39 kcal/mol, 42.93 kcal/mol, 5.92 kcal/mol, 25.49 kcal/mol, 2.85 kcal/mol, respectively. The important π→π* transition is including π(N1-C6)→π*(C2-O8) with stabilization energy ($E^{(2)}$) about 42.93 kcal/mol. The highest resonance energy in compound **SYSA-2** is observed for π*(N1-C6)→π*(C4-C5) transition with stabilization energy about 108.77 kcal/mol. The n→π* transitions have the most resonance energy ($E^{(2)}$) rather than n→σ* transitions that are included in n1(N3)→π*(C2-O8), n1(N3)→π*(C4-C5), n1(N7)→π*(N1-C6) interactions with stabilization energies of 53.10 kcal/mol, 41.97 kcal/mol, 67.40 kcal/mol, respectively. The highest resonance energies for n→σ* transitionsis observed for n1(N1)→σ*(C2-N3), n2(O8)→σ*(N1-C2), n2(O8)→σ*(C2-N3), n2(O20)→σ*(O17-P18), n2(O20)→σ*(P18-O19) interactions with the resonance energies ($E^{(2)}$) 15.34 kcal/mol, 19.97 kcal/mol, 20.53 kcal/mol, 16.37 kcal/mol, 20.04 kcal/mol, respectively.

The results of NBO analysis including the occupation numbers with their energies for the interacting NBOs [interaction between natural bond orbital A and natural bond orbital B (A-B)] and the polarization coefficient values of atoms in the molecule **SYSA-2** are calculated using the B3LYP/6-31G* level of theory is reported in Table 8 (atoms numbering is according to Fig. 1).

Table 8 Calculated natural bond orbitals (NBO) and the polarization coefficient for each hybrid in selected bonds of the molecule **SYSA-2** using the B3LYP/6-31G* level of theory.

Occupancy (a.u.)	Bond (A-B)[a]	Energy (a.u.)	ED_A (%)	ED_B (%)	NBO	S(%) (A)	S(%) (B)	P(%) (A)	P(%) (B)
1.98325	σ(N1-C2)	-0.83453	59.40	40.60	0.7707 ($sp^{1.90}$) + 0.6372 ($sp^{1.77}$)	34.41	36.12	65.41	63.82
1.98228	σ(N1-C6)	-0.84922	58.27	41.73	0.7633 ($sp^{1.74}$) + 0.6460 ($sp^{2.11}$)	36.38	32.13	63.43	67.81
1.75172	π(N1-C6)	-0.31174	69.33	30.67	0.8326 ($sp^{1.00}$) + 0.5538 ($sp^{1.00}$)	0.00	0.00	99.75	99.87
1.98688	σ(C2-N3)	-0.80722	35.25	64.75	0.5937 ($sp^{2.24}$) + 0.8047 ($sp^{2.07}$)	30.85	32.55	69.01	67.42
1.99387	σ(C2-O8)	-1.02965	34.89	65.11	0.5907 ($sp^{2.06}$) + 0.8069 ($sp^{1.53}$)	32.69	39.41	67.21	60.28
1.97259	π(C2-O8)	-0.36948	24.87	75.13	0.4987 ($sp^{99.99}$) + 0.8668 ($sp^{1.00}$)	0.13	0.01	99.63	99.75
1.98337	σ(N3-C4)	-0.84097	62.96	37.04	0.7935 ($sp^{1.86}$) + 0.6086 ($sp^{2.53}$)	34.95	28.32	65.02	71.56
1.97927	σ(C4-C5)	-0.75434	50.33	49.67	0.7094 ($sp^{1.52}$) + 0.7648 ($sp^{1.83}$)	39.67	35.37	60.29	64.59
1.81528	π(C4-C5)	-0.29041	43.28	56.72	0.6579 ($sp^{1.00}$) + 0.7531 ($sp^{1.00}$)	0.01	0.00	99.91	99.94
1.97764	σ(C5-C6)	-0.70736	49.52	50.48	0.7037 ($sp^{2.11}$) + 0.7105 ($sp^{1.68}$)	32.16	37.23	67.79	62.73
1.99201	σ(C6-N7)	-0.86573	40.10	59.90	0.6332 ($sp^{2.28}$) + 0.7740 ($sp^{1.52}$)	30.45	39.62	69.45	60.35
1.98796	σ(C9-O10)	-0.83588	31.78	68.22	0.5637 ($sp^{3.93}$) + 0.8260 ($sp^{2.49}$)	20.23	28.61	79.52	71.32
1.98595	σ(O10-C11)	-0.81410	69.26	30.74	0.8322 ($sp^{2.44}$) + 0.5544 ($sp^{4.55}$)	29.07	17.98	70.87	81.76
1.97620	σ(C11-C12)	-0.61912	51.39	48.61	0.7168 ($sp^{2.63}$) + 0.6972 ($sp^{2.77}$)	27.54	26.53	72.41	73.41
1.99350	σ(C13-O14)	-0.83396	33.85	66.15	0.5818 ($sp^{3.75}$) + 0.8133 ($sp^{2.36}$)	21.01	29.76	78.79	70.16
1.97198	σ(O17-P18)	-0.80995	79.49	20.51	0.8916 ($sp^{2.83}$) + 0.4529 ($sp^{3.28}$)	26.13	22.67	73.83	74.28
1.97727	σ(P18-O19)	-0.82212	21.47	78.53	0.4634 ($sp^{3.15}$) + 0.8862 ($sp^{2.71}$)	23.36	26.95	73.66	72.99
1.97905	σ(P18-O20)	-0.91196	24.52	75.48	0.4951 ($sp^{2.18}$) + 0.8688 ($sp^{2.07}$)	31.00	32.41	67.50	67.04
1.98033	σ(C4-H22)	-0.56476	63.21	36.79	0.7951 ($sp^{2.12}$) + 0.6065 (s)	32.06	100	67.89	-

1.98988	σ(N7-H24)	-0.67055	72.23	27.77	0.8499 ($sp^{2.30}$) + 0.5270 (s)	29.88	100	70.08	-
1.99003	σ(N7-H25)	-0.67762	72.07	27.93	0.8489 ($sp^{3.21}$) + 0.5285 (s)	30.39	100	69.57	-
1.97715	σ(C11-H27)	-0.52207	63.14	36.86	0.7946 ($sp^{2.87}$) + 0.6071 (s)	25.79	100	74.14	-
1.98912	σ(O14-H30)	-0.73606	78.00	22.00	0.8832 ($sp^{2.79}$) + 0.4690 (s)	26.39	100	73.51	-
1.98560	σ(O21-H35)	-0.77174	77.12	22.88	0.8782 ($sp^{3.06}$) + 0.4783 (s)	24.62	100	75.29	-
1.89413	n1(N1)	-0.34268	-	-	$sp^{2.43}$	29.12	-	70.72	-
1.59591	n1(N3)	-0.27907	-	-	$sp^{99.99}$	0.03	-	99.97	-
1.69090	n1(N7)	-0.26626	-	-	$sp^{99.99}$	0.02	-	99.96	-
1.95896	n1(O8)	-0.67423	-	-	$sp^{0.72}$	58.08	-	41.88	-
1.85897	n2(O8)	-0.28069	-	-	$sp^{39.29}$	2.48	-	97.34	-
1.94294	n1(O10)	-0.54812	-	-	$sp^{1.94}$	33.99	-	65.97	-
1.91492	n2(O10)	-0.38453	-	-	$sp^{11.03}$	8.31	-	91.65	-
1.97526	n1(O14)	-0.56443	-	-	$sp^{1.39}$	41.85	-	58.09	-
1.92119	n2(O14)	-0.31746	-	-	$sp^{49.54}$	1.98	-	97.94	-
1.97878	n1(O15)	-0.58865	-	-	$sp^{1.16}$	46.38	-	53.57	-
1.94521	n2(O15)	-0.30188	-	-	$sp^{99.99}$	0.60	-	99.31	-
1.95175	n1(O17)	-0.58432	-	-	$sp^{1.45}$	40.86	-	59.07	-
1.90712	n2(O17)	-0.34089	-	-	$sp^{99.99}$	0.42	-	99.50	-
1.96061	n1(O19)	-0.60590	-	-	$sp^{1.25}$	44.48	-	55.43	-
1.91864	n2(O19)	-0.34056	-	-	$sp^{99.99}$	0.26	-	99.64	-
1.97849	n1(O20)	-0.72764	-	-	$sp^{0.48}$	67.54	-	32.42	-
1.81463	n2(O20)	-0.26945	-	-	$sp^{1.00}$	0.00	-	99.74	-
1.96872	n1(O21)	-0.61243	-	-	$sp^{1.21}$	45.16	-	54.76	-
1.92175	n2(O21)	-0.35010	-	-	$sp^{99.99}$	0.08	-	99.82	-

[a] A-B is the bond between atom A and atom B. (A: natural bond orbital and the polarization coefficient of atom; A-B: natural bond orbital and the polarization coefficient of atom B).

The value of polarization coefficients show the importance of the two hybrids in the formation of bonds in the molecules [24]. The differences in electronegativity of the atoms involved in the bond formation are reflected in the larger differences in the polarization coefficients of the atoms (C-O, C-N, O-P, O-H, C-H bonds). The calculated bonding orbital for the σ(C2-N3) bond is the $\sigma=0.5937(sp^{2.24})+0.8047(sp^{2.07})$ with occupancy 1.98688 a.u. and low energy -0.80722 a.u. The polarization coefficients of the C2=0.5937 and the N3=0.8047 show the importance of N3 atom in forming σ(C2-N3) bond rather than C2 atom. The calculated bonding orbital for the σ(C9-O10) bond is $\sigma=0.5637(sp^{3.93})+0.8260(sp^{2.49})$ with low energy -0.83588 a.u. and high occupancy 1.98796 a.u. The polarization coefficients of C9=0.5637 and O10=0.8260 show large difference in polarization coefficients C9 and O10 atoms in σ(C9-O10); therefore the O10 atom has the most important in forming σ(C9-O10) bond rather than C9 atom. The calculated bonding orbital for the σ(C5-C6) bond is $\sigma=0.7037(sp^{2.11})+0.7105(sp^{1.68})$ with low energy -0.70736 a.u. and high occupancy 1.97764 a.u. The polarization coefficients of C5=0.7037 and C6=0.7105 show low difference in polarization coefficients C5 and C6 atoms in σ(C5-C6) bond and importance of two

atoms in forming the bond. The π(N1-C6) orbital with the calculated bonding $\pi=0.8326(sp^{1.00})+0.5538(sp^{1.00})$ orbital has 69.33% N1 character with $sp^{1.00}$ hybrid and has 30.67% C6 character with $sp^{1.00}$ hybrid. The sp hybrids of N1 and C6 have 99.75% and 99.87% p-character, respectively. Therefore, π(N1-C6) bond participates as the electron donation to π*(C2-O8) orbital in π(N1-C6)→π*(C2-O8) interaction with stabilization energy ($E^{(2)}$) 42.93 kcal/mol (Table 7). Also, the π(C4-C5) orbital with the bonding $\pi=0.6579(sp^{1.00})+0.7531(sp^{1.00})$ orbital has 43.28% C4 character with $sp^{1.00}$ hybrid and has 53.72% C5 character with $sp^{1.00}$ hybrid. The sp hybrids of C4 and C5 have 99.91% and 99.94% p-character, respectively. Therefore, π(C4-C5) bond participates as the electron donation to π*(N1-C6) orbital in π(C4-C5)→π*(N1-C6) transition with resonance energy ($E^{(2)}$) 25.49 kcal/mol (Table 7). According to the results reported in Table 8, the natural hybrid orbital n1(N3) with $sp^{99.99}$ hybrid, high occupancy 1.59591 a.u. and high energy -0.27907 a.u. has p-character (99.97%). The p-type lone pair orbital n1(N3) participates as the electron donation to π*(C2-O8) and π*(C9-N10) at n1(N3)→π*(C2-O8) and n1(N3)→π*(C4-C5) transitions with high stabilization energies ($E^{(2)}$) 53.10 kcal/mol and 41.97 kcal/mol, respectively (Table 7). The natural hybrid orbital n1(N7) with $sp^{99.99}$ hybrid has 99.96% p-character and it acts a electron donation to π*(N1-C6) in n1(N7)→π*(C22-N23) transition with high resonance energies ($E^{(2)}$) 67.40 kcal/mol (Table 7).

3.6. Electronic Structure and Excited States of the Compounds SYSA-1,2,3,4

We used TD-DFT method for predicting the absorption spectra of the compounds **SYSA-1,2,3,4**. The theoretical absorption spectra of the optimized structures were calculated in solvent water using the TDB3LYP/6-31G* method. Excited states (λ = 100-400 nm) considered for the calculation equations that were carried out using the IEFPCM (Integral Equation Formalism PCM) method coupled to UAKS radii and were obtained the exact amount of the maximum absorption wavelength (λ_{max}) to the title molecules.

Compound SYSA-1: According to theoretical electronic absorption spectrum of the compound **SYSA-1** (Table 9), the strong peak apeare at λ_{max} = 173.82 nm and the oscillator strength f = 0.63 that is due to charge transfer of one electron into the excited state $S_0 \rightarrow S_{13}$, which it describes by a wave function corresponding to a superposition of four configurations for one-electron excitation H-3→L+1 (73%), H-4→L+1 (8%), H-3→L (5%), H→L (3%). The main transition is observed from HOMO-3 to LUMO+1 [H-3→L+1 (73%)]. The other important excited state of the compound **SYSA-1** is such as $S_0 \rightarrow S_3$ with f = 0.46, which is appear at 223.68

nm and describes by a wave function corresponding to a superposition of three configurations for one-electron excitations H→L (31%), H→L+1 (62%), H-3→L+1 (3%). Excitation of an electron from H→L+1 (62%) gives the main contribution to the formation of the absorption band at 223.68 nm. (Table 9). The other excited states of the title compound have very small intensity. The calculated UV spectrum of the compound **SYSA-1** is shown in Fig. 5.

Table 9 Electronic absorption spectrum of the compound **SYSA-1** calculated by TDB3LYP/6-31G*

Excited State	Wavelength (nm)	Excitation Energy (eV)	Configurations Composition (corresponding transition orbitals)	Oscillator Strength (f)
$S_0 \rightarrow S_3$	223.68	5.54	H→L (31%), H→L+1 (62%), H-3→L+1 (3%)	0.46
$S_0 \rightarrow S_{13}$	173.82	0.63	H-3→L+1 (73%) H-4→L+1 (8%), H-3→L (5%), H→L (3%)	0.63

*H-HOMO, L-LUMO

**In these tables the transitions with f ≥ 0.10 are presented.

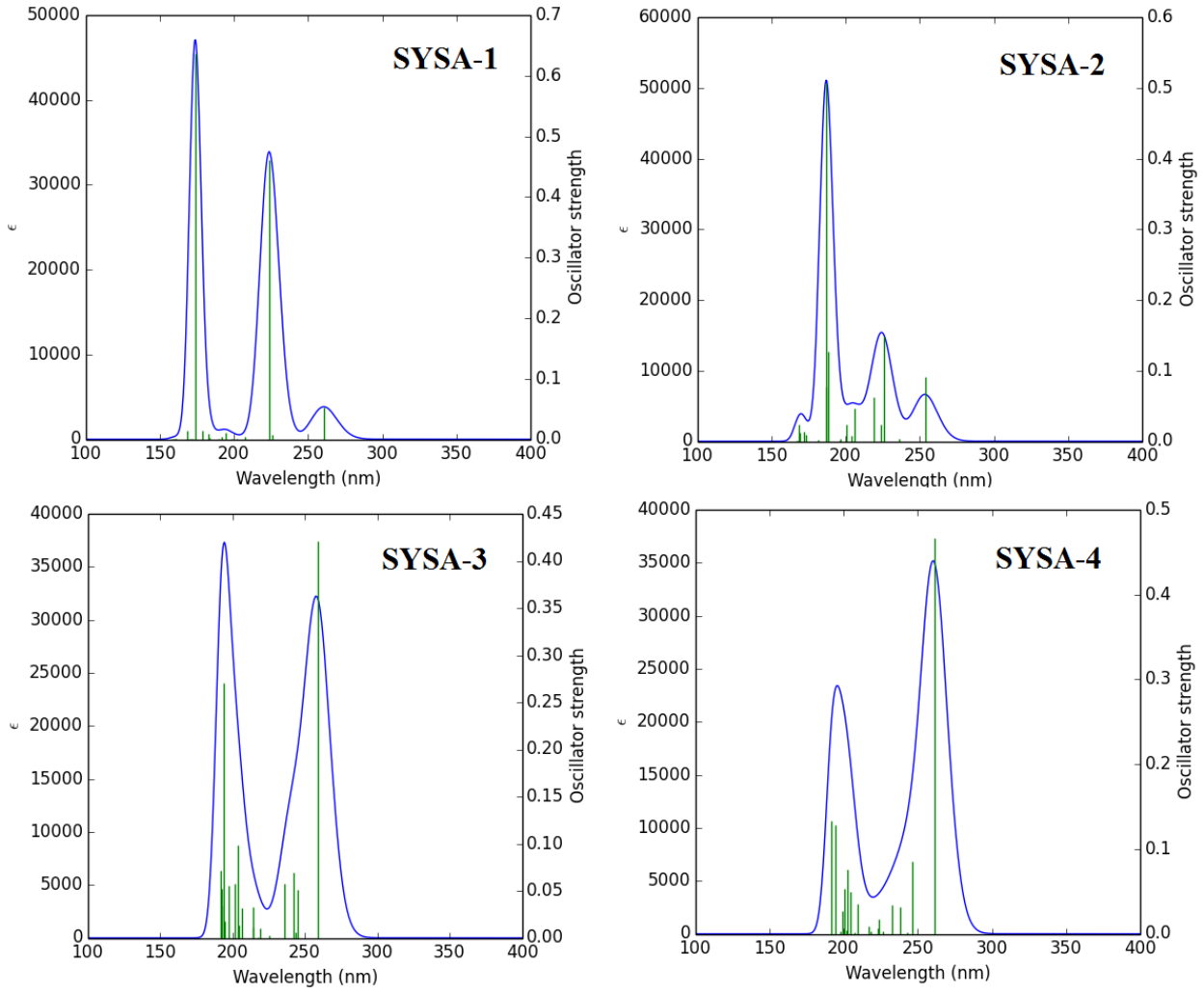

Fig. 5 UV/Vis spectra of the compound **SYSA-1,2,3,4** in the solvent water calculated by TDB3LYP/6-31G* method.

Compound SYSA-2: As can be seen from Table 10, the strong peak at λ_{max} = 186.58 nm and the oscillator strength f = 0.50 in electronic absorption spectrum of the compound **SYSA-2** is due to charge transfer of one electron into the excited state $S_0 \rightarrow S_{13}$, which it describes by a wave function corresponding to a superposition of six configurations for one-electron excitation H-2→L+1 (26%), H-1→L+1 (48%), H→L+1 (10%), H-7→L (4%), H-1→L (2%), H→L (2%). Excitation of an electron from HOMO-1 to LUMO+1 [H-1→L+1 (48%)] gives the main contribution to the formation of the absorption band at 186.58 nm. The other excited states of the title compound have small intensity. The calculated UV spectrum of the compound **SYSA-2** is shown in Fig. 5.

Table 10 Electronic absorption spectrum of the compound **SYSA-2** calculated by TDB3LYP/6-31G*

Excited State	Wavelength (nm)	Excitation Energy (eV)	Configurations Composition (corresponding transition orbitals)	Oscillator Strength (f)
$S_0 \rightarrow S_1$	253.47	4.89	H→L (89%), H-1→L (6%), H-1→L+1 (2%)	0.10
$S_0 \rightarrow S_3$	225.94	5.48	H-4→L (16%), H-1→L (68%), H-3→L (6%), H→L (3%)	0.14
$S_0 \rightarrow S_{11}$	188.27	6.58	H-8→L (20%), H-7→L (44%), H-2→L+1 (11%), H-1→L+1 (13%), H→L+1 (4%)	0.12
$S_0 \rightarrow S_{13}$	186.58	6.64	H-2→L+1 (26%), H-1→L+1 (48%), H→L+1 (10%), H-7→L (4%), H-1→L (2%), H→L (2%)	0.50

*H-HOMO, L-LUMO

**In these tables the transitions with f ≥ 0.10 are presented.

Compound SYSA-3: According to theoretical calculations, the strong peak in electronic absorption spectrum of the compound **SYSA-3** is observed at λ_{max} = 258.76 nm and the oscillator strength f = 0.42 that is due to charge transfer of one electron into the excited singlet state $S_0 \rightarrow S_1$, which it describes by a wave function corresponding to a superposition of two configurations for one-electron excitation H→L (88%), H→L+3 (7%) (Table 11). The main transition is observed from HOMO to LUMO [H→L (88%)]. The other important excited state is excitation of one electron at 193.74 nm (f = 0.27) that belonged to the transition into the state $S_0 \rightarrow S_{17}$ and describes by a wave function corresponding to a superposition of twelve configurations for one-electron excitations H-6→L (10%), H-4→L+1 (10%), H-4→L+3 (16%), H-2→L+2 (12%), H-1→L+3 (11%), H-5→L (8%), H-3→L+1 (3%), H-3→L+2 (4%), H-3→L+3 (5%), H-2→L+3 (3%), H-1→L+2 (4%), H→L+4 (4%). Excitation of an electron from H-4→L+3 (16%) gives the main contribution to the formation of the absorption band at 193.74

nm. The other excited states of the title compound have very small intensity. The calculated UV spectrum of the compound **SYSA-3** is shown in Fig. 5.

Table 11 Electronic absorption spectrum of the compound **SYSA-3** calculated by TDB3LYP/6-31G*

Excited State	Wavelength (nm)	Excitation Energy (eV)	Configurations Composition (corresponding transition orbitals)	Oscillator Strength (f)
$S_0 \rightarrow S_1$	258.76	4.79	H→L (88%), H→L+3 (7%)	0.42
$S_0 \rightarrow S_{13}$	203.65	6.08	H-2→L+2 (14%), H-1→L+1 (61%), H-2→L+1 (6%), H-1→L+2 (8%), H-1→L+3 (4%)	0.10
$S_0 \rightarrow S_{17}$	193.74	6.39	H-6→L (10%), H-4→L+1 (10%), H-4→L+3 (16%), H-2→L+2 (12%), H-1→L+3 (11%), H-5→L (8%), H-3→L+1 (3%), H-3→L+2 (4%), H-3→L+3 (5%), H-2→L+3 (3%), H-1→L+2 (4%), H→L+4 (4%)	0.27

*H-HOMO, L-LUMO

**In these tables the transitions with f ≥ 0.10 are presented.

Compound SYSA-4: As can be seen from Table 12, the strong peak at λ_{max} = 260.99 nm and the oscillator strength f = 0.46 in electronic absorption spectrum of the compound **SYSA-4** is due to charge transfer of one electron into the excited singlet state $S_0 \rightarrow S_1$, which it describes by a wave function corresponding to a superposition of three configurations for one-electron excitation H→L (90%), H→L+2 (3%), H→L+3 (3%). Excitation of an electron from H→L (90%) gives the main contribution to the formation of the absorption band at 260.99 nm. The other excited states of the title compound have small intensity. The calculated UV spectrum of the compound **SYSA-4** is shown in Fig. 5.

Table 12 Electronic absorption spectrum of the compound **SYSA-4** calculated by TDB3LYP/6-31G*

Excited State	Wavelength (nm)	Excitation Energy (eV)	Configurations Composition (corresponding transition orbitals)	Oscillator Strength (f)
$S_0 \rightarrow S_1$	260.99	4.75	H→L (90%), H→L+2 (3%), H→L+3 (3%)	0.46
$S_0 \rightarrow S_{19}$	194.18	6.38	H-7→L (22%), H-4→L+2 (12%), H-3→L+1 (12%), H→L+4 (16%), H-9→L (3%), H-8→L (6%), H-6→L (7%), H-5→L+1 (2%), H-4→L+3 (4%)	0.12
$S_0 \rightarrow S_{20}$	191.97	6.45	H-4→L+1 (25%), H-3→L+1 (12%), H-3→L+2 (25%), H-7→L (4%), H-6→L (3%), H-5→L+2 (3%), H-4→L+2 (5%), H-2→L+2 (3%), H-2→L+3 (6%), H→L+4 (3%)	0.13

*H-HOMO, L-LUMO

**In these tables the transitions with f ≥ 0.10 are presented.

4. Experimental

4.1. DPPH (2,2 diphenyl 1-picryl hydrazyl) or Free radical scavenging method

In this method DPPH (2,2-diphenyl-1-picryl hydrazyl) is the reagent used to analyze the antioxidant activity of the title compounds. DPPH* is a free radical with an unpaired valence

electron, and molecules do not dimerize in either its solid state or in solution. In the solution of DPPH in methanol, the odd electron in the DPPH* free radical results in the formation of purple color, with an absorption band with a maximum at 519 nm. The color turns from purple to yellow as the molar absorptivity of the DPPH* radical at 519 nm reduces from 9660 to 1640 when the odd electron presents in DPPH* radical becomes paired with hydrogen from the antioxidant being studied to form the reduced DPPH-H. The resulting decolorization is stoichiometric with respect to number of electrons captured. Butylated hydroxyl anisole or ascorbic acid can be used as a standard one [36-38].

4.2. ABTS cation radical scavenging activity

The scavenging activity against 2,2 azino-bis (3-ethylbenzothiazloine6-sulfonic acid) (ABTS) cation radical was measured according to the method described [39-41]. ABTS-positive cation radical was produced directly by reacting of 5 mM ABTS solution with 2 mM potassium persulfate and keeping the mixture for 10-12 h. in a dark place at 20 ºC. Prior to the beginning of the assay, ABTS solution was diluted with ethanol to an absorbance of 0.70 + 0.02 at 734 nm. Sample solution (1 mL) was added to ABTS solution (2 mL) and mixed. The sample absorbance was read at 734 nm after 25 min incubation at the room temperature. The ABTS cation radical scavenging activity was expressed as equivalents of Trolox according to the equation obtained from the standard Trolox graph [25].

5. Antioxidative Chemical Assays

5.1. DPPH Radical Scavenging Activity

The 1,1-diphenyl-2-picrylhydrazyl (DPPH) radical scavenging activity of the title compounds was determined at four concentrations ranging from 1 μM to 250 μM (Table 13). The given data show decrease in the concentration of DPPH radical due to the scavenging by the best anthraquinone derivatives. All the studied structures were active in assay, **SYSA-2** showed the highest value for DPPH radical scavenging. This is confirmed by their IC_{50} values that show antioxidant potential decreased in the order of **SYSA-2>SYSA-1>SYSA-4>SYSA-3**.

Table 13. DPPH Radical Scavenging Capacities of BHA and of the Title Compounds

Structures	DPPH Scavenging Activity (%)				
	1 μM	50μM	100μM	250μM	IC_{50} μM
BHA	1.2±1.9	59.9±0.5	65.4±0.40	62.1±3.2	36.5±1.7
SYSA-2	5.3±1.3	10.3±3.0	30.0±1.3	60.1±2.0	10.5±2.3
SYSA-3	3.2±1.5	16.3±1.6	28.7±0.3	47.1±1.6	33.8±1.2
SYSA-1	3.6±2.0	11.7±5.3	44.6±1.3	37.9±1.6	11.2±1.5

SYSA-4	8.3±1.8	18.9±1.2	55.3±0.7	66.0±1.9	19.7±0.8

5.2. ABTS Radical Cation Scavenging Activity

Total antioxidant activity of the compounds was measured using the ABTS radical cation decolorization assay. It is an excellent means for determining the antioxidant activity of hydrogen-donating and of chain-breaking antioxidants [42,43]. The calculated IC_{50} show that **SYSA-2** has high potency in ABTS radical cation scavenging observed with BHA (Table 14).

Table 14. ABTS Radical Cation Scavenging Capacities of BHA and Anthraquinone Derivatives

Structures	DPPH Scavenging Activity (%)				
	1 μM	50μM	100μM	250μM	IC_{50} μM
BHA	1.2±1.9	59.9±0.5	65.4±0.40	62.1±3.2	36.5±1.7
SYSA-2	3.7±1.0	11.4±0.2	33.5±1.1	44.0±1.6	4.4±0.5
SYSA-3	6.2±0.1	15.5±4.7	47.5±2.1	64.3±3.9	16.6±0.3
SYSA-1	3.7±3.0	13.9±1.3	41.9±0.3	39.2±1.7	18.6±1.4
SYSA-4	9.3±1.1	18.3±1.2	51.2±0.7	63.0±1.1	22.7±2.7

6. Conclusions

The four new pyrimidine derivatives (**SYSA-1,2,3,4**) were optimized using Density Functional Theory (DFT/B3LYP/6-31G*). The Eg, global hardness, antioxidant activity of title compounds can be ranged in the following sequence: **SYSA-2**>**SYSA-1**>**SYSA-4**>**SYSA-3**. According to NBO analysis of compound **SYSA-2**, the π-bonds and lone pairs with p-character participates as the electron donation to π*-bonds that lead to high stabilization energy ($E^{(2)}$) and the highest resonance energies in title compound is observed for π*→π* transition. The strongest signals in calculated electronic absorption spectra of the compounds **SYSA-1, SYSA-2, SYSA-3, SYSA-4** are observed at λ_{max} = 173.62, 186.58, 258.76, 260.99 nm. All the studied structures were active in assay, **SYSA-2** showed the highest value for DPPH radical scavenging (10.5±2.3 μM). The calculated IC_{50} show that **SYSA-2** has high potency in ABTS radical cation scavenging observed with BHA (4.4±0.5 μM).

References

[1] D.F.V. Lewis, M.N. Jacobs, M. Dickins, Compound lipophilicity for substrate binding to human P450s in drug metabolism, Drug Discov. Today 9 (2004) 530–537.

[2] J. Cui, L. Liu, D. Zhao, C. Gan, X. Huang, Q. Xiao, B. Qi, L. Yang, Y. Huang, Synthesis, characterization and antitumor activities of some steroidal derivatives with side chain of 17-hydrazone aromatic heterocycle, Steroids 95 (2015) 32–38.

[3] Z. Nasir, A. Ali, M. Shakir, R. Wahab, S. uzzaman, L. Fullah, Silica supported NiO nanocomposite prepared via sol-gel technique and its excellent catalytic performance for one-pot multicomponent synthesis of benzodiazepine derivatives under microwave irradiation, New J. Chem. 41 (2017) 5893–5903.

[4] Y. Deng, Y. Wang, C. Cherian, Z. Hou, S.A. Buck, L.H. Matherly, A. Gangjee, Synthesis and discovery of high affinity folate receptoor-specific glycinamide ribonucleotide formyltransferase inhibitors with antitumor activity, J. Med. Chem. 51 (2008) 5052–5063.

[5] T.E. Renau, C. Kennedy, R.G. Ptak, J.M. Breitenbach, J.C. Drach, L.B. Townsend, Synthesis of non-nucleoside analogs of toyocamycin, sangivamycin, and thiosangivamycin: the effect of certain 4- and 4,6-substituents on the antiviral activity of pyrrolo[2,3-d]pyrimidines, J. Med. Chem. 39 (1996) 3470–3476.

[6] R.J. Gillespie, S.J. Bamford, S. Gaur, A.M. Jordan, J. Lerpiniere, H.L. Mansell, G.C. Stratton, Antagonists of the human A2A receptor. Part 5: highly bio-available pyrimidine-4-carboxamides, Bioorg. Med. Chem. Lett. 19 (2009) 2664–2667.

[7] E.R. Kotb, E.M.H. Morsy, M.M. Anwar, E.M. Mohi El-Deen, H. Awad, New pyrimidine derivatives: Synthesis, antitumor and antioxidant evaluation, Int. J. Pharm. Technol. 7 (2015) 8061–8085.

[8] V. Paresh and E. F. Schroeder, USPatent 2 724 559, C. A. 50 (1956) 11370, 1956.

[9] C. Oliver Kappe, W. M. F. Fabian, and M. A. Semones, Conformational analysis of 4-aryl-dihydropyrimidine calcium channel modulators. A comparison of ab initio, semiempirical and X-ray crystallographic studies, Tetrahedron 53 (1997) 2803–2816.

[10] M. Okabe, R. C. Sun, and G. B. Zenehoff, “Synthesis of 1- (2,3-dideoxy-2-fluoro-.beta.-D-threo-pentofuranosyl)cytosine (F-ddC). A promising agent for the treatment of acquired immune deficiency syndrome, J. Org. Chem. 56 (1991) 4393–4395.

[11] K. Atwal, US Patent 4 769 371, C. A.110 (1989) 114853, 1988.

[12] S. M. Sondhi, S. Jain, M. Dinodia, R. Shukla, and R. Raghubir, “One pot synthesis of pyrimidine and bispyrimidine derivatives and their evaluation for anti-inflammatory and analgesic activities, Bioorg. Med. Chem. 15 (2007) 10 3334–3344.

[13] A. Balkan, M. Ertan, and T. Burgemeister, Synthesis and structural evaluations of thiazolo[3,2-a]pyrimidine derivatives, Arc. Pharm. 325 (1992) 499–501.

[14] S. M. Sondhi, M. Dinodia, R. Rani, R. Shukla, and R. Raghubir, "Synthesis, anti-inflammatory and analgesic activity evaluation of some pyrimidine derivatives, Indian J. Chem. B 48 (2009) 273–281.

[15] M. F. Hasan, A. M. Madkour, I. Saleem, J. M. A. Rahman, and E. A. Z. Mohammed, Reactions of 5-(p-Anisyl)-2-methyl-7- (p-tolyl)-4H-pyrido[2,3-d][1,3]oxazin-4-one, Heterocycles 38 (1994) 57–69.

[16] K. D. Thomas, A. V. Adhikari, and N. S. Shetty, Design, synthesis and antimicrobial activities of some new quinoline derivatives carrying 1,2,3-triazole moiety, Eur. J. Med. Chem. 45 (2010) 3803–3810.

[17] P.G. Parr, W. Yang, Density functional approach to the frontier-electron theory of chemical reactivity, J. Am. Chem. Soc. 106 (1984) 4049–4050.

[18] S. Shahab, L. Filippovich, R. Kumar, M. Darroudi, M. Yousefzadeh Borzehandani, M. Gomar, Photochromic properties of the molecule Azure A chloride in polyvinyl alcohol matrix, J. Mol. Struct. 1101(2015) 109–115.

[19] S. Shahab, H. Alhosseini Almodarresiyeh, R. Kumar, M. Darroudi, A study of molecular structure, UV, IR, and ^{1}H NMR spectra of a new dichroic dye on the basis of quinoline derivative, J. Mol. Struct. 1088 (2015) 105–110.

[20] S. Shahab, L. Filippovich, M. Sheikhi, H. Yahyaei, M. Aharodnikova, R. Kumar, M. Khaleghian, Spectroscopic (Polarization, ExcitedState, FT-IR, UV/Vis and 1H NMR) and Thermophysical Investigations of New Synthesized Azo Dye and Its Application in Polarizing Film, American J. Mater. Synth. Process. 5 (2017) 17–23.

[21] S. Shahab, L. Filippovich, M. Sheikhi, R. Kumar, E. Dikusar, H. Yahyaei, A. Muravsky, Polarization, excited states, trans-cis properties and anisotropy of thermal and electrical conductivity of the 4-(phenyldiazenyl)aniline in PVA matrix, J. Mol. Struct. 1141 (2017) 703–709.

[22] S. Shahab, M. Sheikhi, L. Filippovich, M. Khaleghian, E. Dikusar, H. Yahyaei, M. Yousefzadeh Borzehandani, Spectroscopic Studies (Geometry Optimization, E→Z Isomerization, UV/Vis, Excited States, FT-IR, HOMO-LUMO, FMO, MEP, NBO, Polarization) and Anisotropy of Thermal and Electrical Conductivityof New Azomethine Dyes in Stretched Polymer Matrix, Silicon 10 (2018) 2361–2385.

[23] S. Shahab, M. Sheikhi, L. Filippovich, E. Dikusar, H. Yahyaei, R. Kumar, M. Khaleghian, Design of geometry, synthesis, spectroscopic (FT-IR,UV/Vis, excited state, polarization) and anisotropy (thermal conductivity and electrical) properties of new synthesized derivatives of (*E*,*E*)- azomethines in colored stretched poly (vinyl alcohol) matrix, J. Mol. Struct. 1157 (2018) 536–550.

[24] M. Sheikhi, S. Shahab, L. Filippovich, H. Yahyaei, E. Dikusar, M. Khaleghian, New derivatives of (E,E)-azomethines: Design, quantum chemical modeling, spectroscopic (FT-IR, UV/Vis, polarization) studies, synthesis and their applications: Experimental and theoretical investigations, J. Mol. Struct. 1152 (2018) 368–385.

[25] S. Shahab, M. Sheikhi, R. Alnajjar, L. Filippovich, E. Dikusar, Antitumor and Antioxidant Activities of the New Anthraquinone Derivatives: Synthesis, DPPH, ABTS, Biological and DFT Investigations, Chinese Journal of Structural Chemistry 38 (2019) 1673-1690.

[26] S. Shahab, M. Sheikhi, L. Filippovich, E. Dikusar, M. Rouhani, A. Pazniak, R. Kumar, Molecular Investigations of the New Synthesized Azomethines as Antioxidants: Theoretical and Experimental Studies, Current Mol. Med. 19 (2019) 419-433.

[27] M.J. Frisch, G.W. Trucks, H.B. Schlegel, G.E. Scuseria, M.A. Robb, J.R. Cheeseman, G. Scalmani, V. Barone, B. Mennucci, G.A. Petersson, H. Nakatsuji, M. Caricato, X. Li, H.P. Hratchian, A.F. Izmaylov, J. Bloino, G. Zheng, J.L. Sonnenberg, M. Hada, M. Ehara, K. Toyota, R. Fukuda, J. Hasegawa, M. Ishida, T. Nakajima, Y. Honda, O. Kitao, H. Nakai, T. Vreven, J.A. Montgomery, Jr., J.E. Peralta, F. Ogliaro, M. Bearpark, J.J. Heyd, E. Brothers, K.N. Kudin, V.N. Staroverov, R. Kobayashi, J. Normand, K. Raghavachari, A. Rendell, J.C. Burant, S.S. Iyengar, J. Tomasi, M. Cossi, N. Rega, J.M. Millam, M. Klene, J.E. Knox, J.B. Cross, V. Bakken, C. Adamo, J. Jaramillo, R. Gomperts, R.E. Stratmann, O. Yazyev, A.J. Austin, R. Cammi, C. Pomelli, J.W. Ochterski, R.L. Martin, K. Morokuma, V.G. Zakrzewski, G.A. Voth, P. Salvador, J.J. Dannenberg, S. Dapprich, A.D. Daniels, Ö. Farkas, J.B. Foresman, J.V. Ortiz, J. Cioslowski, D.J. Fox, Gaussian 09 revision A02,Gaussian, Inc., Wallingford CT, 2009.

[28] S. Shahab, M. Sheikhi, L. Filippovich, Z. Ignatovich, A. Muravsky, R. Alnajjar, S. Kaviani, A. Strogova, Optimization, Spectroscopic (FT-IR, Excited States, UV/Vis) Studies, FMO, ELF, LOL, QTAIM and NBO Analyses and Electronic Properties of Two New Pyrimidine Derivatives, Chinese J. Struct. Chem. 38 (2019) 1615-1639.

[29] M. Sheikhi, D. Sheikh, A. Ramazani, Three-component synthesis of electron-poor alkenes using isatin derivatives, acetylenic esters, triphenylphosphine and theoretical study, S. Afr. J. Chem. 67 (2014) 151–159.

[30] A. Frisch, A.B. Nielson, A.J. Holder,GAUSSVIEW User Manual, Gaussian Inc., Pittsburgh, PA; 2000.

[31] S. Shahab, M. Sheikhi, L. Filippovich, E. DikusarAnatol'evich, H. Yahyaei, Quantum chemical modeling of new derivatives of (E,E)-azomethines: Synthesis, spectroscopic (FT-IR, UV/Vis, polarization) and thermophysical investigations, J. Mol. Struct. 1137 (2017) 335–348.

[32] H. Yahyaei, S. Shahab, M. Sheikhi, L. Filippovich, H. A.Almodarresiyeh, R. Kumar, E. Dikusar, M. Yousefzadeh Borzehandan, R. Alnajjar, Anisotropy (optical, electrical and thermal conductivity) in thin polarizing films for UV/Vis regions of spectrum: Experimental and theoretical investigations, Spectrochimica Acta Part A: Mol. Biomol. Spectrosc. 192 (2018) 343–360.

[33] M. Sheikhi, S. Shahab, M. Khaleghian, M. Ahmadianarog, R. Kumar, Investigation of the Adsorption Rubraca Anticancer Drug on the CNT(4,4-8) Nanotube as a Factor of Drug Delivery: A Theoretical Study Based on DFT Method, *Current Mol. Med.* 19 (2019) 473-486.

[34] M. Sheikhi, S. Shahab, M. Khaleghian, R. Kumar, Interaction Between New Anti-cancer Drug Syndros and CNT(6,6-6) Nanotube for Medical Applications: Geometry Optimization, Molecular Structure, Spectroscopic (NMR, UV/Vis, Excited state), FMO, MEP and HOMO-LUMO Investigation, Appl. Surf. Sci. 434 (2018) 504–513.

[35] F. Weinhold, C.R. Landis, Neutral Bond Orbitals and Extensions of Localized; 2001.

[36] P.R. Parry, C. Wang, A.S. Batsanov, M.R. Bryce, B. Tarbit, Functionalized pyridylboronic acids and their Suzuki cross-coupling reactions to yield novel heteroarylpyridines, J. Org. Chem. 67 (2002) 7541–7543.

[37] J. Murray, P. Politzer, The Electrostatic Potential: An Overview WIREs, Comput. Mol. Sci. 1 (2011) 153–163.

[38] F. Proutiere, M. Aufiero, F. Schoenebeck, Reactivity and stability of dinuclear Pd(I) complexes: Studies on the active catalytic species, insights into precatalyst activation and deactivation, and application in highly selective cross-coupling reactions, J. Am. Chem. Soc. 134 (2011) 606–612.

[39] M. Joshaghani, M. Daryanavard, E. Rafiee, S. Nadri, Synthesis and applications of a new palladacycle as a high active catalyst in the Suzuki couplings, J. Organomet. Chem. 693 (2008) 3135–3140.

[40] M. Mora, C. Jimenez-Sanchidrian, J.R. Ruiz, Suzuki cross-coupling reactions over Pd(II)-hydrotalcite catalysts in water, J. Mol. Catal. A Chem. 285 (2008) 79–83.

[41] D. Zim, S.M. Nobre, A.L. Monteiro, Suzuki cross-coupling reaction catalyzed by sulfur-containing palladacycles: Formation of palladium active species, J. Mol. Catal. A Chem. 287 (2008) 16–23.

[42] T. Rasheed, N. Rasool, M. Noreen, Y. Gull, M. Zubair, A. Ullah, U.A. Rana, Palladium(0) catalyzed Suzuki cross-coupling reactions of 2,4-dibromothiophene: Selectivity, characterization and biological applications, J. Sulfur Chem. 36 (2015) 240–250.

[43] R. Re, N. Pellegrini, A. Proteggente, A. Pannala, M. Yang, C. Rice-Evans, Antioxidant activity applying an improved ABTS radical cation decolorization assay, Free Rad. Biol. Med. 26 (1999) 1231–1237.